University of Pennsylvania
ScholarlyCommons

Departmental Papers (CBE)

Department of Chemical & Biomolecular Engineering

December 2007

Hydrogen Production via CH_4 and CO Assisted Steam Electrolysis

Wensheng Wang
University of Pennsylvania

John M. Vohs
University of Pennsylvania, vohs@seas.upenn.edu

Raymond J. Gorte
University of Pennsylvania, gorte@seas.upenn.edu

Follow this and additional works at: https://repository.upenn.edu/cbe_papers

Recommended Citation

Wang, W., Vohs, J. M., & Gorte, R. J. (2007). Hydrogen Production via CH_4 and CO Assisted Steam Electrolysis. Retrieved from https://repository.upenn.edu/cbe_papers/101

Postprint version. Published in *Topics in Catalysis*, Volume 46, Issue 3-4, December 2007, pages 380-385.
Publisher URL: http://dx.doi.org/10.1007/s11244-007-9005-8

This paper is posted at ScholarlyCommons. https://repository.upenn.edu/cbe_papers/101
For more information, please contact repository@pobox.upenn.edu.

Hydrogen Production via CH_4 and CO Assisted Steam Electrolysis

Abstract

Porous composite anodes consisting of a yttria-stabilized zirconia (YSZ) backbone that was impregnated with CeO_2 and various amounts of metallic components including Cu, Co and Pd were fabricated. The performance of these anodes was then tested in a solid oxide water electrolysis cell under conditions where the anode was exposed to the reducing gasses H_2, CH_4 and CO. The reducing gasses were used to decrease the electrochemical potential of the cell and increase overall efficiency. The results of this study show that Cu-CeO_2-YSZ anodes have low catalytic activity for the oxidation of CO and CH_4 and are not very effective in lowering the cell potential while operating in the reducing gas assisted mode. The addition of Co to the Cu-CeO_2- YSZ anode resulted in a modest increase in the catalytic activity and enhanced the thermal stability of the anode. A Pd-C-CeO_2-YSZ anode was found to have the highest catalytic activity of those tested and gave the largest reductions in the operating potential of the solid oxide electrolysis cell.

Keywords

solid oxide electrolyzer, hydrogen production, CH4, CO, depolarization

Comments

Postprint version. Published in *Topics in Catalysis*, Volume 46, Issue 3-4, December 2007, pages 380-385.
Publisher URL: http://dx.doi.org/10.1007/s11244-007-9005-8

This journal article is available at ScholarlyCommons: https://repository.upenn.edu/cbe_papers/101

Hydrogen Production via CH_4 and CO Assisted Steam Electrolysis

Wensheng Wang, John M. Vohs, and Raymond J. Gorte*

Department of Chemical and Biomolecular Engineering
University of Pennsylvania
Philadelphia, PA 19104

Abstract

Porous composite anodes consisting of a yttria-stabilized zirconia (YSZ) backbone that was impregnated with CeO_2 and various amounts of metallic components including Cu, Co and Pd were fabricated. The performance of these anodes was then tested in a solid oxide water electrolysis cell under conditions where the anode was exposed to the reducing gasses H_2, CH_4 and CO. The reducing gasses were used to decrease the electrochemical potential of the cell and increase overall efficiency. The results of this study show that Cu-CeO_2-YSZ anodes have low catalytic activity for the oxidation of CO and CH_4 and are not very effective in lowering the cell potential while operating in the reducing gas assisted mode. The addition of Co to the Cu-CeO_2-YSZ anode resulted in a modest increase in the catalytic activity and enhanced the thermal stability of the anode. A Pd-C-CeO_2-YSZ anode was found to have the highest catalytic activity of those tested and gave the largest reductions in the operating potential of the solid oxide electrolysis cell.

*Corresponding author: gorte@seas.upenn.edu; Key words: solid oxide electrolyzer, hydrogen production, CH_4, CO, depolarization.

Introduction

The proposed hydrogen economy in which fuel cells will play a major role as energy conversion devices will require the development of efficient methods for the production of hydrogen. While most hydrogen is currently produced by the steam reforming of methane, this approach has the drawback of not being particularly amenable to a highly distributed H_2 production infrastructure and also does not employ non greenhouse gas producing energy sources such as nuclear, hydroelectric, wind, or solar. Electrolysis of water is an alternative method for H_2 production that may alleviate some of the drawbacks of more conventional hydrogen production methods. Solid oxide electrolyzers (SOE) are particularly attractive since their high temperature of operation has both kinetic and thermodynamic advantages [1-3]. A SOE is essentially a solid oxide fuel cell (SOFC) that is operated in reverse and most prototype SOEs are constructed of same materials as those used in SOFCs: yttiria-stabilized zirconia (YSZ) as the electrolyte, a Ni-YSZ ceramic-metallic (cermet) composite as the H_2-H_2O electrode, and an electronically conducting perovskite such as Sr-doped $LaMnO_3$ (LSM) as the air electrode.

While hydrogen production using SOEs powered by electricity from non-greenhouse gas producing sources is attractive, this approach is currently significantly more expensive than steam reforming of methane. Recently the concept of natural gas assisted electrolysis (NGASE) has been suggested as a method to increase the efficiency of SOEs allowing them to compete more favorably with steam reforming of methane [1-2, 4]. NGASE is a hybrid approach in which the energy required to electrolyze water to produce hydrogen is supplied both by electricity and by the oxidation of a fuel. In a conventional SOE the oxygen ions that are transported through the electrolyte react to produce gaseous oxygen on the anode. The anode is typically exposed to air and this causes open circuit voltage of the cell to be ~1 volt at 700ºC.

This Nernst potential represents the thermodynamic barrier that must be overcome in order to produce H_2 and, therefore, relatively high potentials are required to generate hydrogen in an SOE causing the conversion efficiency to be low. In an NGASE system this thermodynamic potential is greatly reduced by exposing the anode to natural gas or methane which can react directly with the oxygen ions to produce CO_2 and water. Other reducing gasses such as CO or higher hydrocarbons can also be used [1-2]. When using methane as the reducing gas the overall reaction for the SOE cell is the same as that for methane steam reforming. The SOE cell has the advantage however in that it produces humidified H_2 which can be used directly in a PEM fuel cell as opposed to a conventional methane steam reforming system which produces a stream containing H_2, CO_2, H_2O and small amounts of CO and CH_4.

While the operation of an NGASE system has been demonstrated, little effort has gone into optimizing the catalytic properties of the anode for this application. Conventional Ni-cermet anodes that are used in SOFCs cannot be used in an NGASE system since they are prone to coking when exposed to hydrocarbons [5-6]. We have previously reported on the development of Cu-CeO_2-based anodes for SOFCs that do not promote coking when exposed to hydrocarbons allowing hydrocarbon-based fuels to be used directly in the fuel cell without the need for reforming to produce hydrogen [7-8]. The use of such anodes in an NGASE cell has not previously been investigated and is the subject of the work reported here. Specifically we have investigated the electrochemical performance of Cu-CeO_2-YSZ and Cu-Co-CeO_2-YSZ composite anodes in a SOE cell in which H_2, CO, and CH_4 were used as reducing gasses to lower the electrochemical potential of the anode.

Experimental

The solid oxide electrolysis cells used in this investigation were constructed using a three-layer YSZ (8 mole % yttria) disc which consisted of a dense YSZ electrolyte layer sandwiched between two porous electrode layers. The multi-layer disc was fabricated by laminating three YSZ tapes. The center electrolyte tape contained only YSZ and organic binders, while sacrificial pore formers (graphite and/or polyethylene) were also included in the tapes used for the anode and cathode. The tapes were laminated under a pressure of 6 MPa at 340 K and then fired at 1823 K. During firing the pore formers combusted resulting in a dense, 50 μm thick YSZ electrolyte disc 1.25 cm in diameter sandwiched between 50 μm and 300 μm thick porous YSZ layers. The active components of both the anode and cathode were added using wet impregnation as has been described in detail previously [9-15]. The 300-μm thick porous cathodes were loaded with CeO_2, Cu and Co by impregnation of aqueous solutions of $Ce(NO_3)_3$ $Cu(NO_3)_2$ and $Co(NO_3)_2$. The following three anode compositions were used in this study: (1) 15 wt % CeO_2, 30 wt% Cu, (2) 15-wt% CeO_2, 15 wt% Cu, 15 wt% Co, and (3) 15-wt% CeO_2, 1 wt% Pd. Each electrode had an active area of 0.35 cm^2. More detailed descriptions of these electrodes and their characteristics are given in previous publications [9-15].

Electrical contacts were made using Au wire and Au paste on both electrodes except for the Pd-CeO_2-YSZ electrode where Ag paste was used. The cells were sealed onto 1.0 cm diameter alumina tubes using a ceramic adhesive (Aremco, Ultra-Temp 516) with the cathode on the inside of the tube. This tube was then placed into a second larger tube that was sealed at one end. This two-tube set-up allowed the composition and flow rates of the gasses exposed to both electrodes to be carefully controlled. The experimental setup is illustrated in Figure 1. During electrolysis cell testing the anode was exposed to a stream containing 20 % H_2 and 80 % H_2O with a flow rate of 150 ml/min and the anode was exposed to streams of humidified (3 % H_2O)

H_2, CO, or CH_4 which also had a flow rate of 150 ml/min. During testing the cell and associated hardware was placed in a tube furnace with the temperature being monitored using a thermocouple that was positioned 1cm from the cell.

Impedance data were recorded in the galvanostatic mode using a Gamry Instruments potentiostat, with a frequency range from 0.01 Hz to 100 kHz and perturbation amplitude of 5 mV for various dc polarizations. V-i curves were measured in the potentiostat mode over a potential range from 0.3 to -1 V.

Results and Discussion

Performance data obtained at 973 K for the SOE cell with the Cu-CeO_2-YSZ anode exposed to humidified H_2, CO, and CH_4 are presented in Figure 2. As noted in the experimental section, the Co-CeO_2-YSZ cathode was exposed to a stream containing 20% H_2O and 80% H_2 during all of the performance tests. V-i curves are presented in part (a) of the figure while impedance spectra, collected for both negative (electrolysis mode) and positive (fuel cell mode) polarizations, are displayed in parts (b) and (c) for H_2 and CH_4 reducing gasses, respectively..

The experimentally determined open circuit voltages and the theoretical Nernst potentials for the various fuels at 973 and 1073 K are tabulated in Table 1. As shown in this table and in Figure 2a the open-circuit voltage (OCV) at 973 K when exposing the anode to humidified H_2 (3 % H_2O) was -86 mV and increased to -90 mV at 1073 K. These values are only slightly greater than those predicted by the Nernst equation (–88 and -97 mV). This demonstrates the quality of the seals used in the testing system and that there were no leaks between the anode and cathode compartments. Using H_2 as the reducing gas on the anode of an SOE is obviously not practical but it does provide a base case for comparison to the data for CO and CH_4. Since H_2 is relatively

easy to oxidize one would expect only minimal kinetic resistances on the anode when operating with H_2 as the reducing gas. The impedance data in Figure 2b show that this is indeed the case. The arc in the impedance spectra is due to the combined impedance of the anode and cathode. When operating with humidified H_2 at a current density of -140 mA/cm^2 the overall area specific resistance (ASR) of the electrodes is 0.4 Ω cm^2. If one assumes that the impedance of the two electrodes are roughly equal, which is a reasonable assumption when running the cell with both electrodes exposed to H_2/H_2O mixtures, the ASR of the anode is only 0.2 Ω cm^2 at 973 K. Also note that the electrode impedance exhibits only a relatively weak dependence on current density which is consistent with the fact that V-i curve is nearly linear. This result demonstrates that while operating the Cu-CeO_2-YSZ anode with humidified H_2, the kinetics of the anode reaction does not limit the cell performance.

In contrast to the data for humidified H_2, the OCVs for humidified CO and CH_4 are significantly higher than those predicted by the Nernst equation. For example, the measured OCV for CO at 973 K is -63 mV which is 32 mV higher than the Nernst value. The difference for CH_4 is substantially larger where the experimental value is +35 mV compared to the Nernst value of -400 mV. These results indicate that for these fuels the anode reactions, *i.e.* $CO + O^{2-} \rightarrow CO_2 + 2\ e^-$ and $CH_4 + 4\ O^{2-} \rightarrow CO_2 + 2\ H_2O + 8\ e^-$, are not approaching equilibrium. This is not surprising since the Cu-CeO_2-YSZ anode would be expected to have relatively low catalytic activity. This conclusion is also consistent with the V-i curves in Figure 2a which show that there are higher overpotentials when exposing the anode to CO or CH_4, relative to H_2. The fact that the low catalytic activity of the anode is limiting performance is also evident in the impedance spectra while operating on humidified CH_4 as shown in Figure 2c. At 973 K the open circuit electrode ASR is ~0.9 Ω cm^2 for CH_4 which is over four times that obtained for H_2. Also note

that the electrode impedance for CH_4 is a function of current density and increase to over 1 Ω cm^2 at a current density of -140 mA/cm^2. This dependence of the electrode ASR on current density causes the V-i curve to be non-linear as shown in Figure 2a.

The impedance data in Figures 2b and c show some variability in the ohmic loss of the cell (the ohmic loss is given by the high-frequency intercept of the impedance spectrum with the Z_{imag} axis). It was observed that the ohmic loss was found to increase somewhat with the time on stream. While the ohmic loss is generally associated with the resistance of the electrolyte layer it also includes contributions from the electrodes. In our previous studies of SOFCs we have found that the Cu in Cu-CeO_2-YSZ electrodes slowly sinters over time and that this causes a small increase in the ohmic loss of the cell [16-17]. The increase in the ohmic loss observed in the present study can, therefore, be attributed to this sintering process.

The addition of Co to the Cu-CeO_2-YSZ anodes was studies as a means to increase both their catalytic activity and thermal stability. Since Co has low solubility in Cu, the metal layers in these anodes are largely phase separated and due to its lower surface free energy the Cu tends to coat the surface of the Co phase [12-13]. Since unlike Co, Cu is not prone to coking when exposed to hydrocarbons, the layered structure of the Cu-Co bi-metallic anodes imparts a high degree of coking resistance to the bimetallic anodes, while the higher melting temperature of Co compared to Cu provides thermal stability. Some Co still remains exposed on the surface, however, and will likely enhance the catalytic activity as has been suggested in previous studies of similar anodes in SOFCs [12-13]. Results obtained for an SOE cell with a Co/Cu-CeO_2-YSZ anode are presented in Figure 3. While less pronounced than in the previous SOFC study, the addition of Co to the Cu/CeO_2 anodes did produce some improvement in the anode performance when operating the SOE cell on CH_4. This is evident as a decrease in the OCV values for CH_4 at

both 973 and 1073 K (see Table 1). Note, however, that the OCVs are still far from the Nernst potential suggesting that the kinetic limitations are still significant and that equilibrium is not being established. The impedance data for CH_4 at 973 K also show only a modest 0.1 Ω cm^2 improvement in the electrode ASR upon the addition of Co (see Figures 2c and 3c). The addition of Co had an even smaller effect on the performance when using CO as the reducing gas on the anode. For this reducing gas the V-i curves and ASRs were comparable with and without Co. These results demonstrate that the addition of Co to the Cu/CeO_2 anode resulted in only a slight enhancement in the catalytic activity for the electro-oxidation of CO and CH_4. While long term stability was not a major focus of the present investigation the ohmic resistances of the cell with the $Co\text{-}Cu\text{-}CeO_2$ anode were found to be more stable over time compared to that of cell with the $Cu\text{-}CeO_2$ anode suggesting that Co does help to depress Cu sintering in the anode as has been reported in previous studies [12-13].

The results obtained for the cells with the $Cu\text{-}CeO_2$ and $Co\text{-}Cu\text{-}CeO_2$ anodes provide further demonstration of the use of a reducing gas to decrease the oxygen fugacity at the anode and the electrical energy required to pump oxygen through the cell. The poorer performance of the anode when using humidified CH_4 or CO as the reducing gas compared to humidified H_2 indicates, however, that the kinetics of the oxidation reactions on the anode still limit performance and that a higher H_2 production rate at a constant applied potential could theoretically be obtained if the catalytic activity of the anode was improved. Since noble metals, such as Pd, supported on ceria are known to be excellent oxidation catalysts, one might expect significantly enhanced performance if small amounts of Pd were added to the anode. Unfortunately the alloying of Pd with Cu would significantly decrease its effectiveness as a catalyst if it were added to the Cu/CeO_2 or $Co/Cu/CeO_2$ anodes. We have shown in previous

studies, however, that precious metals supported on ceria can be used as the catalyst in SOFC anodes when a carbon film rather than Cu is used to provide electronic conductivity [18]. The performance of Pd-CeO_2-C-YSZ anodes while operating in the electrolysis mode using CO or CH_4 as the reducing gas has not previously been studied. Their performance as anodes in an electrolyzer in which the anode is exposed to a reducing gas was therefore also investigated in the present study.

A SOE cell with a Pd-CeO_2-C-YSZ anode was fabricated by first preparing a cell with an anode containing 1 wt % Pd and 15 wt % CeO_2 using the wet impregnation techniques described above. The cell was then placed in the testing rig and prior to performance evaluation a carbon film was deposited on the anode by exposing it to flowing butane at 973 K for 20 mins. At this temperature pyrolysis of a small fraction of the butane initiates radical chain reactions in the gas phase that produce a highly aromatic carbon residue that condenses on the anode surface. The carbonaceous film produced in this manner is relatively stable and electronically conducting allowing it to be used as the current collector in the anode.

Performance data for the SOE cell with the Pd-CeO_2-C-YSZ composite anode is displayed in Figure 4 and the OCV values are presented in Table 1. The V-i data in Fig. 4a show a dramatic improvement especially for CH_4 compared to that for the cells with the Cu-CeO_2 and Cu-Co-CeO_2 anodes. For example, while using humidified CH_4 as the reducing gas, an applied potential of 0.5 volts produced a current of -0.25 A/cm^2 in the cell with the Cu-CeO_2-YSZ anode, and -0.45 A/cm^2 in the cell with the Pd-CeO_2-C-YSZ anode. This corresponds to an 80% increase in the H_2 production rate on the cathode, while simultaneously decreasing the electrical power input by 80 %. The impedance data while operating with H_2 (Fig. 4b) and CH_4 (Fig. 4c) show that the combined ASRs of the electrodes for CH_4 decreased to 0.3 $\Omega \cdot cm^2$ from

~1.0 $\Omega \cdot cm^2$ for the cells with the Cu or Co-Cu-based anode. This result further demonstrates the enhancement of the catalytic activity for hydrocarbon oxidation upon addition of Pd to the anode.

Finally it is interesting to consider the shape of the V-i curves near open circuit. For all three cells used in this study the V-i curves are linear as they pass from negative polarization during electrolysis mode to positive polarization during fuel cell mode. This is the expected result if the anode and cathode reactions are both reversible and that equilibrium is obtained at OCV. For operation when both electrodes exposed to H_2/H_2O mixtures it is easy to envision how the reactions could be reversible and the fact that the OCVs approach the Nernst values confirms that the reactions are near equilibrium. For the other reducing gases, however, the reactions are clearly not reversible. For example, since CH_4 does not contain oxygen it obviously cannot be the oxygen source during positive (fuel cell) polarization. For these conditions the 3% water in the methane is the oxygen source. In light of this, it is surprising that the V-i curve is linear as you pass through OCV since there is a change in the chemical reactions that are taking place. While the origin of this behavior is not clear it is possible that reaction of the methane or CO with steam to produce a small amount of H_2 may be influencing the V-i characteristics of the cell. Production of hydrogen on the anode during operation in electrolysis mode would also serve to increase the OCV values when operating with humidified CO or CH_4 which is consistent with the high OCV values observed experimentally for these fuels.

Conclusions

The results of this study further demonstrate the concept of exposing the anode of a SOE to a reducing gas in order to decrease the electrochemical potential required for the electrolysis

of water to produce hydrogen. Cu-CeO_2-YSZ composite anodes were found to have low catalytic activity and caused relatively small decreases in the OCV of the cell when they were exposed to CO or CH_4. The addition of Co to the anodes Cu-CeO_2-YSZ increased their thermal stability and enhanced the catalytic activity somewhat. Of the anodes studied, Pd-C-CeO_2-YSZ was found to have the highest catalytic activity and gave the largest reductions in the OCV of the SOE cell. Even for this formulation, however, the oxidation of CH_4 on the anode was far from equilibrium and the reduction in the OCV was significantly less than the theoretical value.

Acknowledgements

This work was funded by the U.S. Department of Energy's Hydrogen Fuel Initiative (grant DE-FG02-05ER15721).

References

1. H.S. Spacil and C.S. Tedmon, Jr., J. Electrochem. Soc. 116 (1969) 1618.
2. H.S. Spacil and C.S. Tedmon, Jr. J. Electrochem. Soc. 116 (1969) 1627.
3. W. Doenitz, R. Schmidberger, E. Steinheil, and R. Streicher, Int. J. Hydrogen Energy 5 (1980) 55.
4. J. Martinez-Frias, A.-Q. Pham, and S.M. Aceves, Int. J. Hydrogen Energy 28 (2003) 483.
5. C.M. Chun, J.D. Mumford and T.A. Ramanarayanan, in: SOFC VI, eds. S.C. Singhal and M. Dokiya, Electrochemical Society Proceedings Series PV 1999-19, p 621.
6. C.H. Toh, P.R. Munroe, D.J. Young and K. Foger, Mater. High Temp. 20 (2003) 129.
7. S. Park, J,M, Vohs and R.J. Gorte, Nature 404 (2000) 265.
8. R.J. Gorte, S. Park, J, M, Vohs and C.Wang, Adv. Materials 12 (2000) 1465.
9. Y. Huang, J. M. Vohs and R. J. Gorte, J. Electrochem. Soc. 151 (2004) A646.
10. Y. Huang, J. M. Vohs and R. J. Gorte, J. Electrochem. Soc. 151 (2004) A1592.
11. Y. Huang, J. M. Vohs and R. J. Gorte, J. Electrochem. Soc. 152 (2005) A1347.
12. S.-I. Lee, J.M. Vohs and R.J. Gorte, J. Electrochem. Soc. 151 (2004) A1319.
13. S.-I. Lee, K. Ahn, J.M. Vohs and R.J. Gorte, Electrochem. Solid-State Lett. 8 (2005) A48.
14. S. McIntosh, J.M Vohs and R.J.Gorte, Electrochem. Solid-State Lett. 6 (2003) A240.
15. O. Costa-Nunes, R J. Gorte and J.M. Vohs, J. Power Sources, 141 (2005) 241.
16. S. McIntosh, J.M Vohs,and R.J. Gorte, J. Electrochem. Soc. 150 (2003) A470.
17. S. Jung, C. Lu, H. He, K. Ahn, R.J. Gorte and J.M. Vohs, *J. Power Sources*, 154 (2006) 42.
18. S. McIntosh, J.M. Vohs and R.J.Gorte, Electrochem. Solid-State Lett. 6 (2003) A240.

Table 1. OCV data for H_2, CO, and CH_4 using different electrode at 973 and 1073 K

Temperature	Fuel	Open Circuit Voltage			
		Co-CeO_2-YSZ	Co-Cu-CeO_2-YSZ	Pd-C-CeO_2-YSZ	Calculated
973 K	H_2	-86 mV	-89 mV	-90 mV	-88 mV
	CO	-63 mV	-44 mV	-74 mV	-94.9 mV
	CH_4	35 mV	27 mV	21 mV	-400 mV
1073 K	H_2	-90 mV	-94 mV	-92 mV	-97 mV
	CO	-68 mV	-46 mV	-29 mV	-99.3 mV
	CH_4	65 mV	28 mV	18 mV	-558 mV

Figure Captions:

Figure 1. Picture and schematic diagram of the SOE test cell.

Figure 2. Performance data at 973 K for the SOE cell with a Cu-CeO_2-YSZ anode. (a) V-i curves for the anode exposed to humidified H_2, CO, CH_4, and impedance spectra with the anode exposed to (b) humidified H_2 and (c) humidified CH_4 at (∇) OCV and current densities of (○) −140 mA/cm^2 and (□) 140 mA/cm^2.

Figure 3. Performance data at 973 K for the SOE cell with a CoCu-CeO_2-YSZ anode. (a) V-i curves for the anode exposed to humidified H_2, CO, and CH_4, and impedance spectra with the anode exposed to (b) humidified H_2 and (c) humidified CH_4 at current densities of (○) −140 mA/cm^2 and (□) 140 mA/cm^2.

Figure 4. Performance data at 973 K for the SOE cell with a C-Pd-CeO_2-YSZ anode. (a) V-i curves for the anode exposed to humidified H_2, CO, and CH_4, and impedance spectra with the anode exposed to (b) humidified H_2 and (c) humidified CH_4 at (∇) OCV and current densities of (○) −140 mA/cm^2 and (□) 140 mA/cm^2.

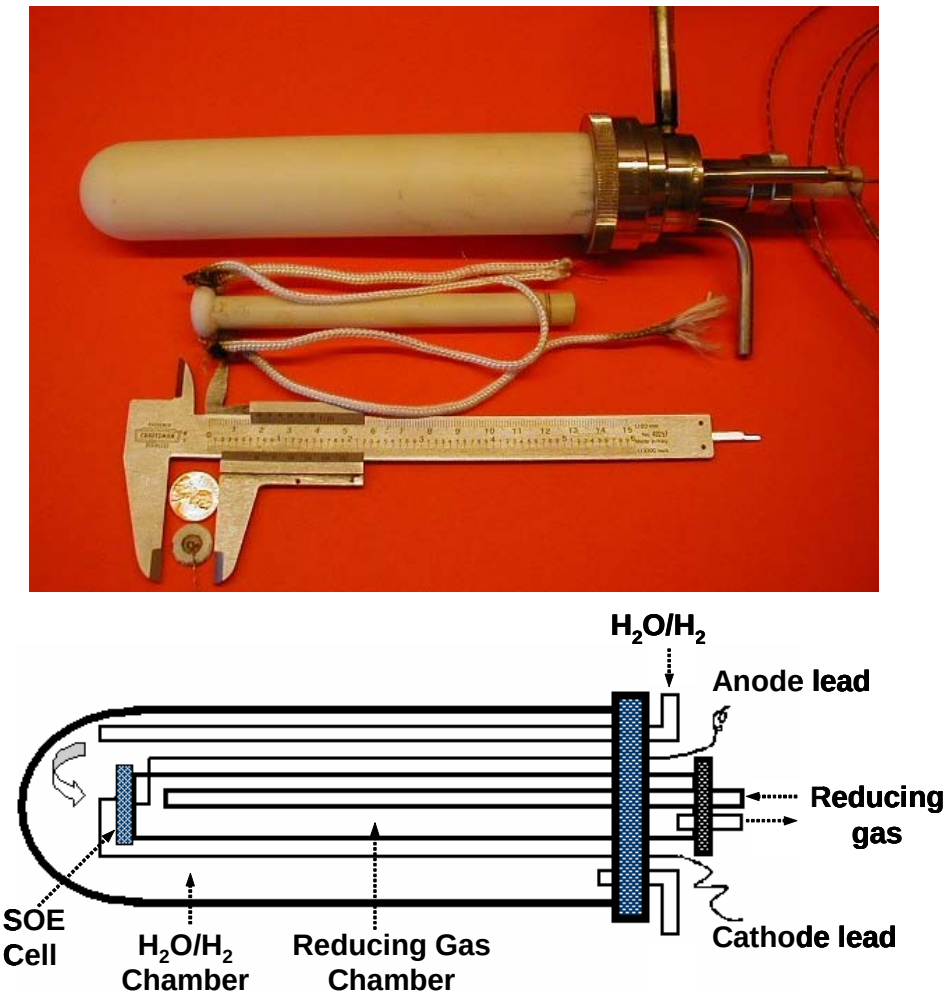
H_2O/H_2
Anode lead
Reducing gas
Cathode lead
SOE Cell
H_2O/H_2 Chamber
Reducing Gas Chamber

Figure 1.

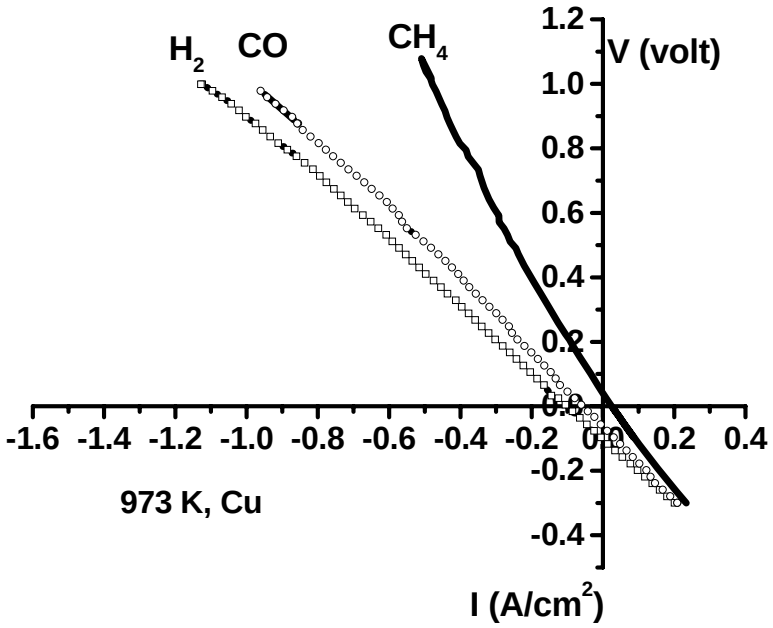

Figure 2a

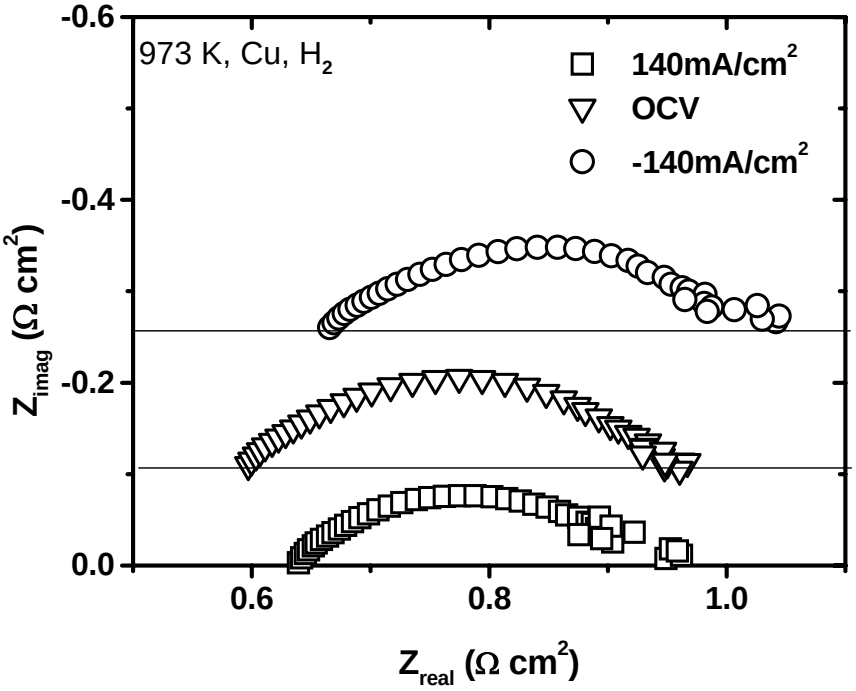

Figure 2b

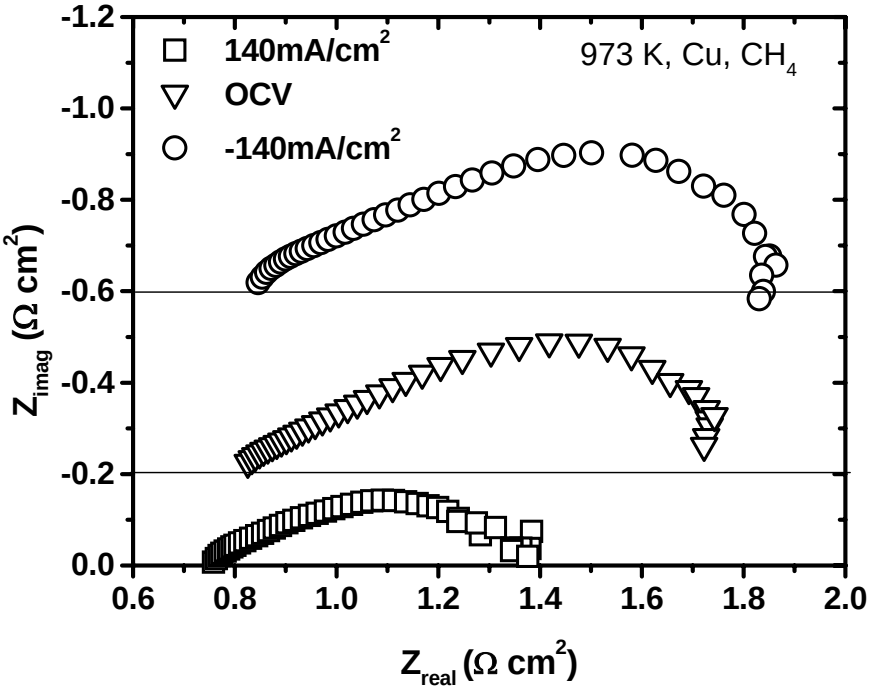
140mA/cm2
OCV
-140mA/cm2
973 K, Cu, CH4
-1.2
-1.0
-0.8
-0.6
-0.4
-0.2
0.0
0.6
0.8
1.0
1.2
1.4
1.6
1.8
2.0
Zimag (Ω cm2)
Zreal (Ω cm2)

Figure 2c

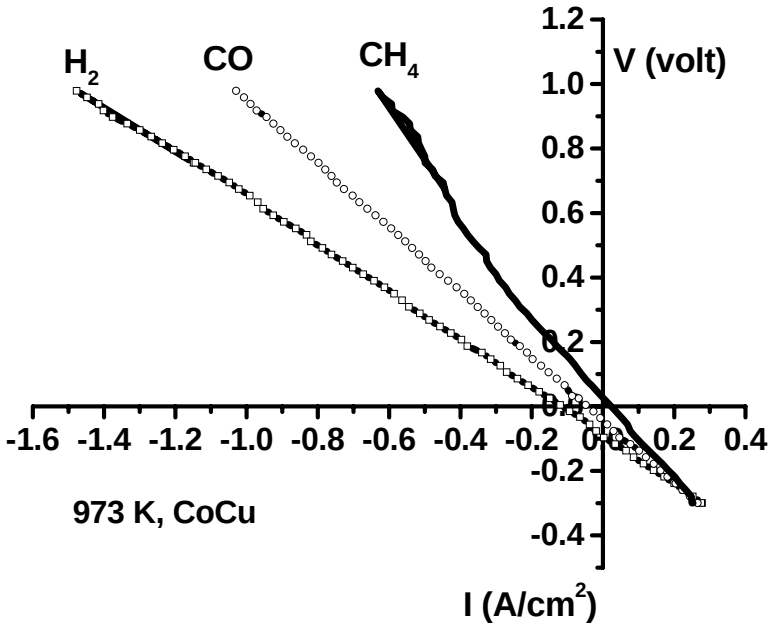

Figure 3a

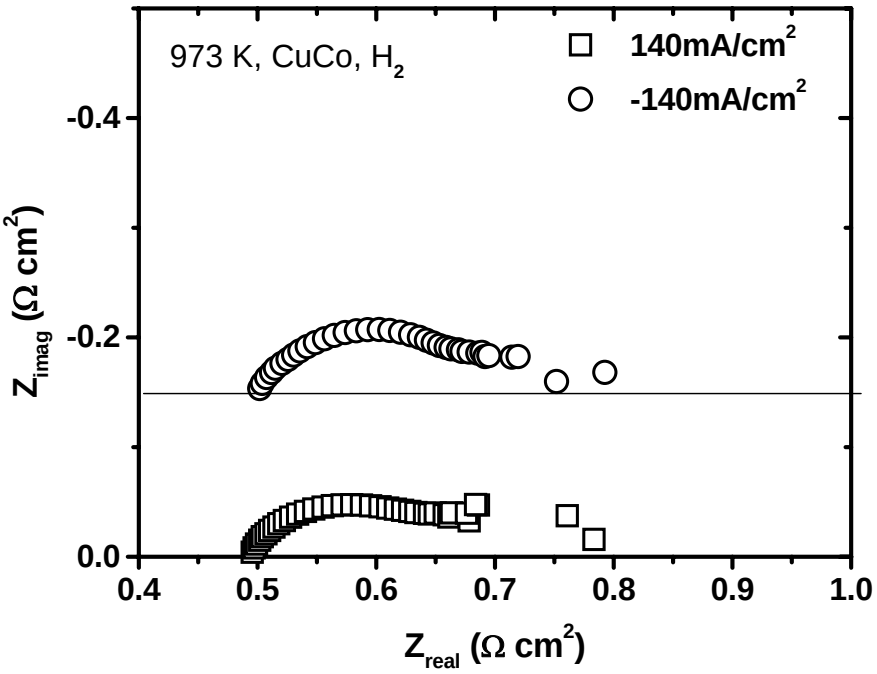

Figure 3b

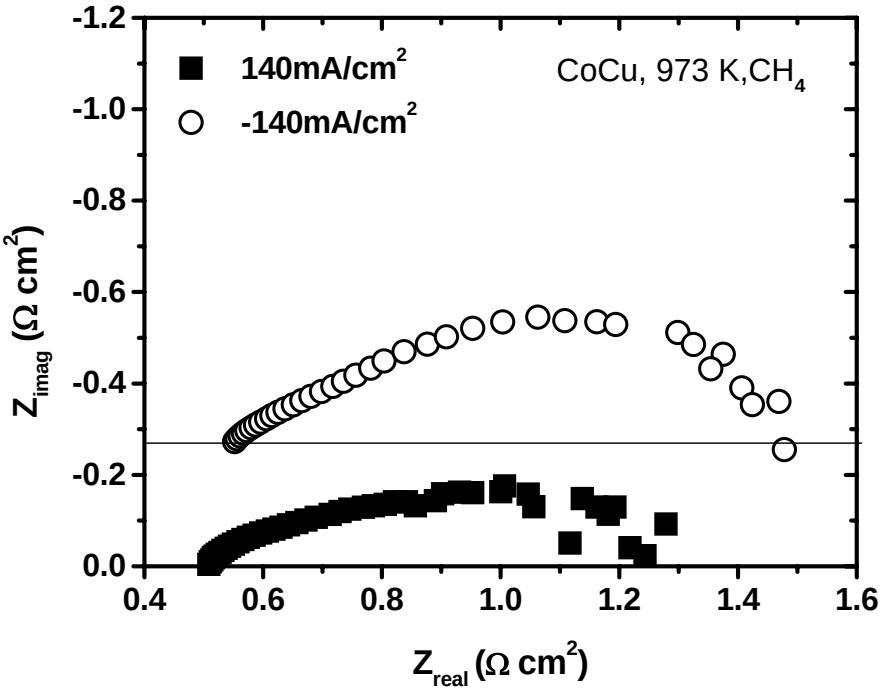
140mA/cm2
-140mA/cm2
CoCu, 973 K,CH4
-1.2
-1.0
-0.8
-0.6
-0.4
-0.2
0.0
0.4
0.6
0.8
1.0
1.2
1.4
1.6
Zimag (Ω cm2)
Zreal (Ω cm2)

Figure 3c

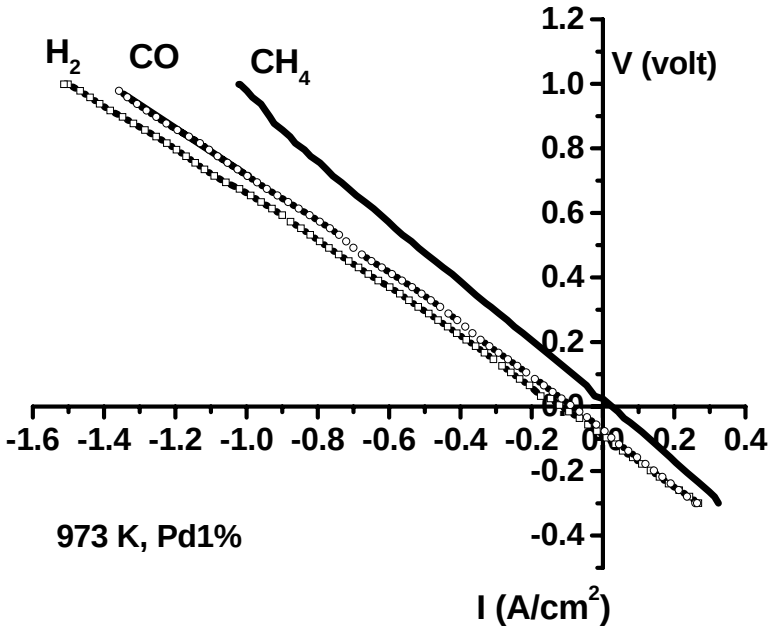

Figure 4a

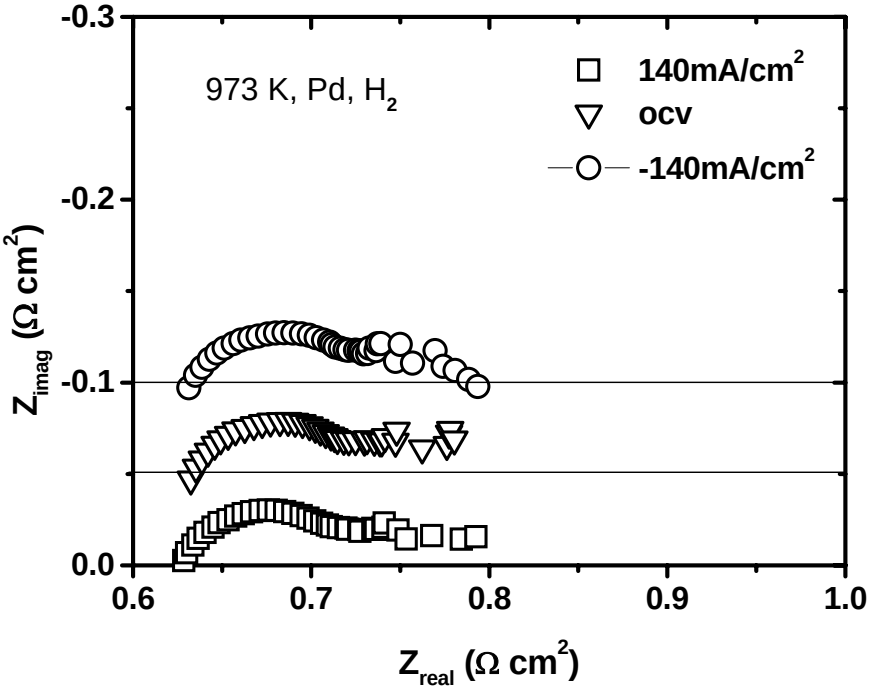

Figure 4b

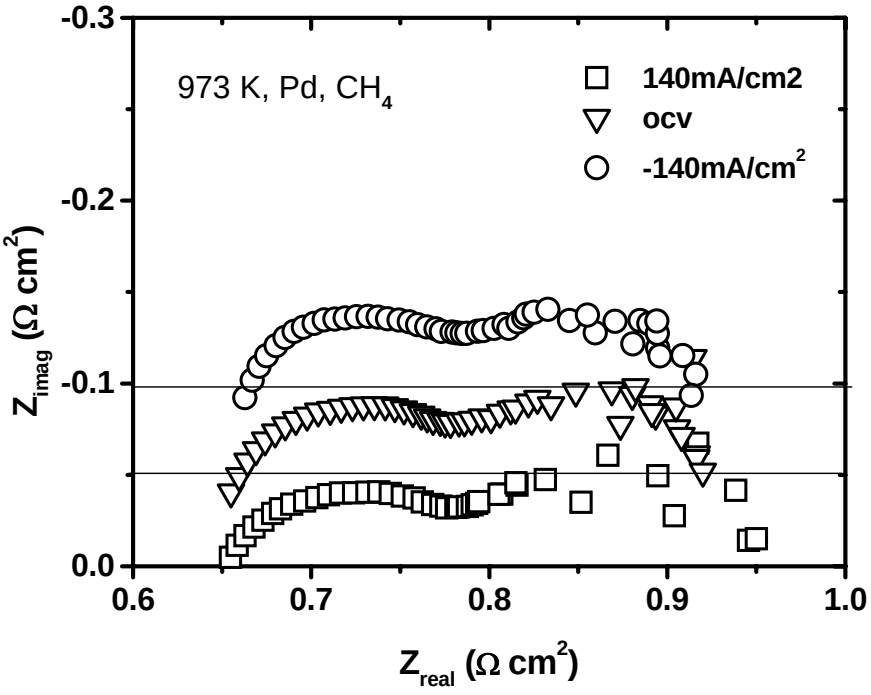
973 K, Pd, CH4
140mA/cm2
ocv
-140mA/cm2
-0.3
-0.2
-0.1
0.0
0.6
0.7
0.8
0.9
1.0
Zimag (Ω cm2)
Zreal (Ω cm2)

Figure 4c